Laser ablation of organic materials for discrimination of bacteria in an inorganic background

Matthieu Baudelet, [1,a] Myriam Boueri,[a] Jin Yu,[2,a] Xianglei Mao,[b]
Samuel S. Mao,[b] and Richard Russo[b]
[a]Université de Lyon, F-69622, Lyon, France, Université Lyon 1, Villeurbanne, CNRS, UMR5579, LASIM
[b]Lawrence Berkeley National Laboratory, Berkeley, California, USA

ABSTRACT

We demonstrate in this paper that laser ablation allows efficient analysis of organic and biological materials. Such analysis is based on laser-induced breakdown spectroscopy (LIBS) which consists in the detection of the optical emission from the plasma induced by a high intensity laser pulse focused on the sample surface. The optimization of the ablation regime in terms of laser parameters (pulse duration, wavelength, fluence) is important to generate a plasma suitable for the analysis. We first present the results of a study of laser ablation of organic samples with different laser parameters using time-resolved shadowgraph. We correlate the early stage expansion of the plasma to its optical emission properties, which allows us to choose suitable laser parameters for an efficient analysis of organic or biological samples by LIBS. As an illustration of the analytical ability of LIBS for biological materials, we show that the emission from CN molecules can be used to distinguish between biological and inorganic samples. Native CN molecular fragment directly ablated from a biological sample are identified using time-resolved LIBS. Those due to recombination with nitrogen contained in atmospheric air can be distinguished with their specific time evolution behavior.

Keywords: Laser-induced plasma, Laser-induced breakdown spectroscopy**,** Organic materials**,** Biological material detection, Bacteria

1. INTRODUCTION

Laser-induced breakdown spectroscopy (LIBS) has been demonstrated as a powerful analytical technique for various types of samples, gas, aerosols, soils, minerals, or alloys.[1,2] The extension of this technique to analysis of organic or biological materials still remains a challenging task, although several groups demonstrated the potentials of LIBS for detection and identification of explosives or biological hazards. [3-8] A crucial step for such extension is certainly a detailed understanding of the laser ablation plasma induced from organic or biological materials. The mechanisms of mass transfer from sample to plasma as well as the interaction between plasma and ambient air need to be extensively studied in order to extract, from emission spectra, suitable analytical data for characterizing the analyzed sample. These mechanisms can sensitively dependent on the parameters of the laser pulses focused on the sample. Compared to the analysis of metallic samples, the analysis of organic samples with LIBS under atmospheric pressure is much more sensitive to interaction between the plasma and the ambient air, since such interaction leads to interfering emissions from organic elements and compounds such as O, N, or CN resulting from the dissociation of air molecules or the recombination between plasma and air. [9,10]

In this paper, we report the study of laser ablation of a typical organic sample, nylon 6,6 using the time-resolved shadowgraph and time-resolved LIBS. The ablations were performed in atmospheric air in order to take into account the interaction between the plasma and the ambient gas. The high time resolution of the shadowgraph allowed us to observe the early stage expansion of the plasma in air, which is highly correlated to the absorption of the laser pulse by the

[1] Actual address : CREOL, The College of Optics & Photonics, University of Central Florida, P.O. Box 162700, Orlando, FL 32816-2700, USA.
[2] Corresponding author: e-mail address: jin.yu@lasim.univ-lyon1.f

Ultrafast Phenomena in Semiconductors and Nanostructure Materials XIII,
edited by Kong-Thon Tsen, Jin-Joo Song, Markus Betz, Abdulhakem Y. Elezzabi,
Proc. of SPIE Vol. 7214, 72140J · © 2009 SPIE · CCC code: 0277-786X/09/$18 · doi: 10.1117/12.808485

sample as well as that by the induced plasma in the case of nanosecond laser ablation. Through a detailed study of the plasma in different ablation regimes, the purpose of this study is to identify a suitable regime for an optimized LIBS analysis of organic or biological materials. The time scale of plasma evolution was divided into two parts: from the impact of the laser pulse on the sample surface to several tens of nanoseconds, the early stage of plasma expansion was observed by time-resolved shadowgraph. Time-resolved LIBS was then used to observe the evolution of spectral emission, especially the emission from diatomic molecular radicals such as CN, from the plasma up to several μs. Continuous observation over these two time intervals allows us to correlate the early stage expansion and the interaction with ambient air of the plasma to its spectral emission detected in LIBS. Different regimes of ablation in terms of laser pulse duration (nanosecond or femtosecond), wavelength (IR or UV) and fluence are systematically studied and compared in order to identify suitable ablation regimes to improve the analytical capability of LIBS for organic or biological materials using molecular emission spectroscopy. The applications of LIBS for the analysis of organic and biological material are illustrated in this paper by the discrimination of bacteria with respect to inorganic materials.

2. EARLY STAGE EXPANSION OF THE PLASMA AND ITS OPTICAL EMISSION PROPERTIES

2.1 Experimental setup

In our experiments, Nylon 6,6 was used as a typical organic sample because it contains native CN molecular radicals. For a biological sample, native CN radicals can be used as a marker for its speciation thanks to its strong emission around 388 nm. However, in a LIBS spectrum of an organic material, the contribution of native CN radicals ablated from the sample has to be distinguished from that of CN radicals due to recombination between plasma and ambient air.[9,11] Nylon presents also good mechanical properties for sample preparation with a good quality flat surface.

Early stage plasma expansion was observed using a time-resolved pump-probe shadowgraph setup. In the nanosecond regime, the ablation beam was provided by a 10 Hz Nd:YAG laser which emitted in the fundamental (1064 nm) or in the fourth harmonic (266 nm). Pulse energy ranged from 1 mJ to 5 mJ with pulse duration of 4 ns. A quartz lens of focal length 50 mm focused the laser pulses on the surface of the sample. The position of the laser beam waist was carefully adjusted in order to obtain a beam size of 100 μm in diameter on the sample surface. Ablation craters were measured using a white light interferometer (Zygo, NewView 200) to confirm that the beam was the same diameter when laser parameters (wavelength, energy) were changed. The resulted fluences ranged from 12.7 J/cm^2 to 63.7 J/cm^2. For the femtosecond ablation regime, a 10 Hz chirped pulse amplification (CPA) Ti:Sapphire laser (800 nm) was used in the same fluence range with a pulse duration of 100 fs.

The probe beam crossed the ablation beam at a right angle. It consisted of one part of the beam provided by the CPA Ti:Sapphire laser. Pulses of about 10 μJ energy were doubled to 400 nm by passing through a KDP crystal. Natural divergence of the beam allowed it to cross the plasma plume with an enlarged section in such way that the plasma was illuminated with a uniform blue beam. Detection of the shadow induced by the plasma was performed using a CCD camera equipped with a narrow band blue filter.

The synchronization between ablation and probe pulses was realized in the nanosecond ablation regime with electronic delay between the Q-switches of the nanosecond laser and the regenerative amplifier of the femtosecond laser. Due to the uncertainty of pulse ejection time with respect to the Q-switch of the regenerative amplifier, actual delay between the nanosecond ablation pulse and the femtosecond probe pulse was measured with two fast photodiodes detecting scattered light from nano and femtosecond pulses. A fast oscilloscope measured the time delay between the two electric pulses corresponding to the two laser pulses for each ablation event. In the femtosecond ablation regime, delay for the probe pulse was generated with an optical delay line. The pump-probe shadowgraph was able to observe the expansion of the plasma from its initiation to a delay of several tens of ns with a time resolution of several nanoseconds for the nanosecond ablation regime (limited by the response time of the photodiodes used). The time resolution for the femtosecond ablation configuration was in the picosecond range.

From about 100 ns after the laser impact on the sample surface up to a delay of several μs, optical emission from the plasma was detected with time-resolved LIBS. The setup used was a typical LIBS setup with a detection system including an Echelle spectrometer coupled to an ICCD camera. Electronic gating on the ICCD allowed a time resolution of 10 ns. In our experiments, nylon samples cut from a same piece of Nylon 6,6 were ablated with laser pulses with

different parameters (pulse duration, wavelength, and energy). Shadowgraph pictures corresponded to single shot images, while time-resolved LIBS signals were accumulated over 200 laser shots to increase the signal to noise ratio. The sample was moved during the measurements in order to ensure a fresh surface for each laser shot.

2.2 Early stage expansion of the plasmas induced in different laser ablation regimes

Fig. 1 shows shadowgraphs of plasmas induced on the surface of a nylon sample by nanosecond IR (1064 nm) laser pulses, with pulse energies of 1, 3 and 5 mJ (Fig. 1 a, b, c respectively) corresponding to fluences of 12.7 J/cm^2, 38.1 J/cm^2 and 63.7 J/cm^2. The corresponding shadowgraphs for nanosecond UV (266 nm) ablation are shown in Fig. 2.

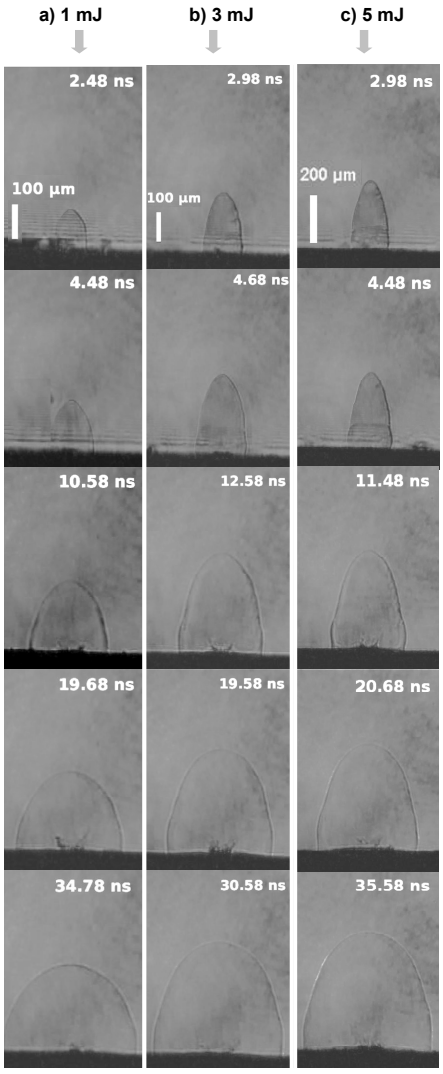

Fig. 1. Shadowgraphs of the plasmas induced on the surface of a nylon sample by nanosecond IR (1064 nm) laser pulses, with pulse energies of 1, 3 and 5 mJ (Fig. 1a, 1b and 1c respectively).

Comparing shockwave expansion of these two ablation regimes, we remark that in the UV regime, shockwaves globally expand in spherical wave for weak as well for high fluences. Shockwave expansion in the IR regime is clearly anisotropic. Expansion backward along the laser pulse propagation direction is faster than transversal expansion. The anisotropy becomes more pronounced when the laser pulse energy increases. This anisotropic expansion behavior in the IR regime is due to the laser-supported detonation wave (LSD).[12] The expanding plasma absorbs energy from the tailing part of the laser pulse, leading to a preferential expansion of the shockwave toward the incoming laser pulse direction.

For a given electronic density, this absorption is more efficient for an infrared pulse due to the dependence of the plasma frequency on electron density. In the UV ablation regime, no significant absorption of the laser pulse by the plasma is observed. The shockwave globally expands in an isotropic way.

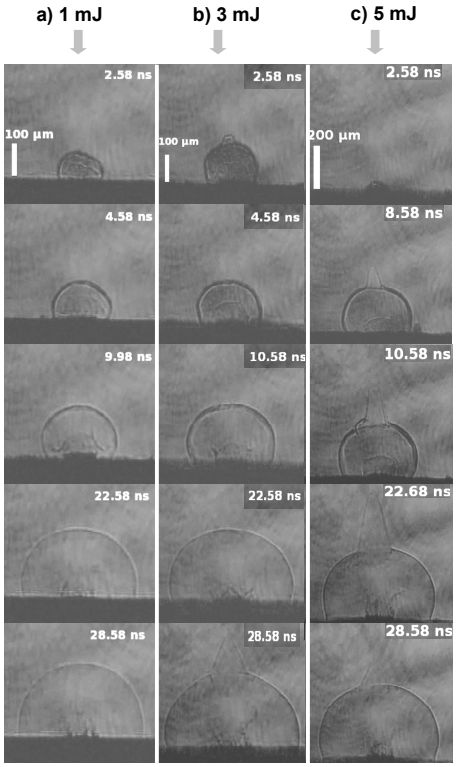

Fig. 2. Shadowgraphs of the plasmas induced on the surface of a nylon sample by nanosecond UV (266 nm) laser pulses, with pulse energies of 1, 3 and 5 mJ (Fig. 2a, 2b and 2c respectively).

We remark in Fig. 2 small structures observed for laser pulse energy larger than 3 mJ on the top of spherically expanding shockwaves in the form of a small tip of higher propagation velocity. The appearance of these picks is not regular pulse to pulse. However the tendency is a more frequent appearance for higher laser energies. This structure is quite different from the LSD observed in Fig. 1 for nanosecond IR ablation. Only a small zone on the top of shockwave is affected. And this structure can appear long time after the end of the laser pulse. Because of the high transparency of the plasma for UV radiation, these local picks can not be due to absorption of laser energy by the plasma. They can however be due to ionized channels induced in air by UV laser pulses before hitting the sample surface. In fact, the probability of photoionization of air molecules (O_2 and N_2) by 266 nm radiation (4.66 eV) becomes important for high laser fluences. The ionization potentials are respectively 12.08 eV and 15.58 eV for O_2 and N_2,[13] which correspond for 266 nm radiation to respectively 3 and 4 photon-transitions. In our experiments, ionized channels become strong enough to be clearly observed by shadowgraph in the UV ablation regime for laser pulse energy larger than 5 mJ. Free electrons from photoionization absorb energy from laser pulse, which leads to heating and transversal expansion of the ionized channel. Propagation of the shockwave is thus accelerated in contact with the ionized channel with lower pressure, which results in a small pick observed on the top of the shockwave. The small size of the high velocity picks is due to the nonlinear power dependence of multiphoton absorption probability, which allows high transition rate only in the central part of laser beam section where laser intensity is higher.

Fig.3 shows shadowgraphs of plasmas induced on the surface of a nylon sample by femtosecond IR (800 nm) laser pulses, with pulse energies of 1, 3 and 4 mJ (Fig. 3 a, b, c respectively). We remark that the observed shockwave expansions are essentially spherical. That corresponds well to the fact that in the femtosecond ablation regime there is not post ablation interaction between the plasma and the laser pulse. However high intensity of a femtosecond laser pulse

can induce an ionized channel in air before the pulse hits the sample. Such channel can be clearly observed in Fig. 3 b) and c) for pulse energy of 3 and 4 mJ. Due to the ionized channel in air, a tip is observed on the top of a shockwave similar to that observed in the nanosecond UV ablation regime. Compared to shadowgraphs in nanosecond ablation regimes, we can also remark that the shadowgraphs in the femtosecond ablation regime present a higher contrast, which corresponds to a plume with higher density.

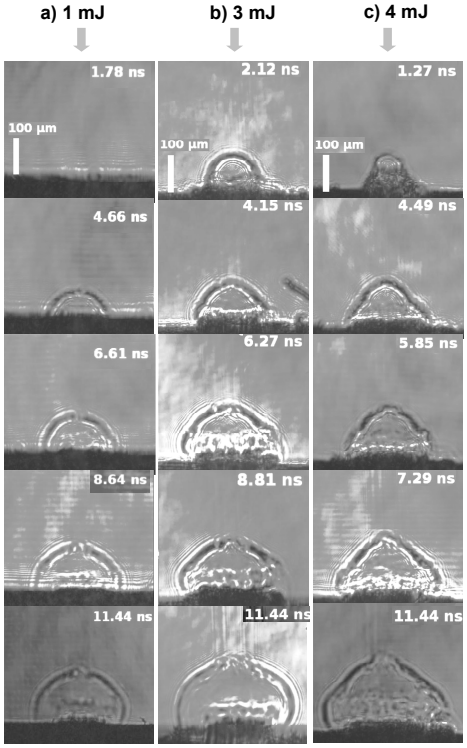

Fig. 3. Shadowgraphs of the plasmas induced on the surface of a nylon sample by femtosecond IR (800 nm) laser pulses, with pulse energies of 1, 3 and 4 mJ (Fig. 3a, 3b and 3c respectively)).

2.3 Time-resolved observation of molecular emission from the plasma

The subsequent evolution of the plasma from a delay of about 100 ns to several µs is monitored by time-resolved LIBS. Fig. 4 shows the results of time-resolved observation of the emission from diatomic molecules CN in plasma. Intensity of the band head at 388.3 nm is measured as a function of the delay after the laser pulse impact on the sample for three different regimes of ablation: nanosecond IR (Fig. 4a), nanosecond UV (Fig. 4b), and femtosecond (Fig. 4c), and for three laser pulse energies (1, 3 and 5 mJ). The intensity of the atomic carbon line at 247.9 nm is also plotted in the figure for comparison. Plasma emission was detected for the different ablation regimes in the same condition.

For the intensity of the carbon line, only one type of behavior is observed: the line intensity monotonically decreases although the decay time constant increases as laser pulse energy increases. However the line intensity of CN molecule exhibits two different types of behavior. In different ablation regimes, molecular line intensity can monotonically decrease, or undergo an initial increasing phase before a subsequent decay. We have demonstrated in our previous works that monotonic intensity decay indicates the emission from native CN molecules directly ablated from the sample. Such native CN molecules can be used as a marker of biological materials or organic materials containing CN radicals like nylon.[9] The initial increase of emission intensity from CN molecules indicates the contribution from the recombination between atomic or molecular carbon in the plasma and nitrogen molecules in air. Such recombination has been observed in different circumstances.[11,14-18] Recombination time constant of several hundreds of nanoseconds can be well fitted by considering involved chemical reactions $C_2 + N_2 \rightarrow 2CN$ and $2C + N_2 \rightarrow 2CN$.[14,15]

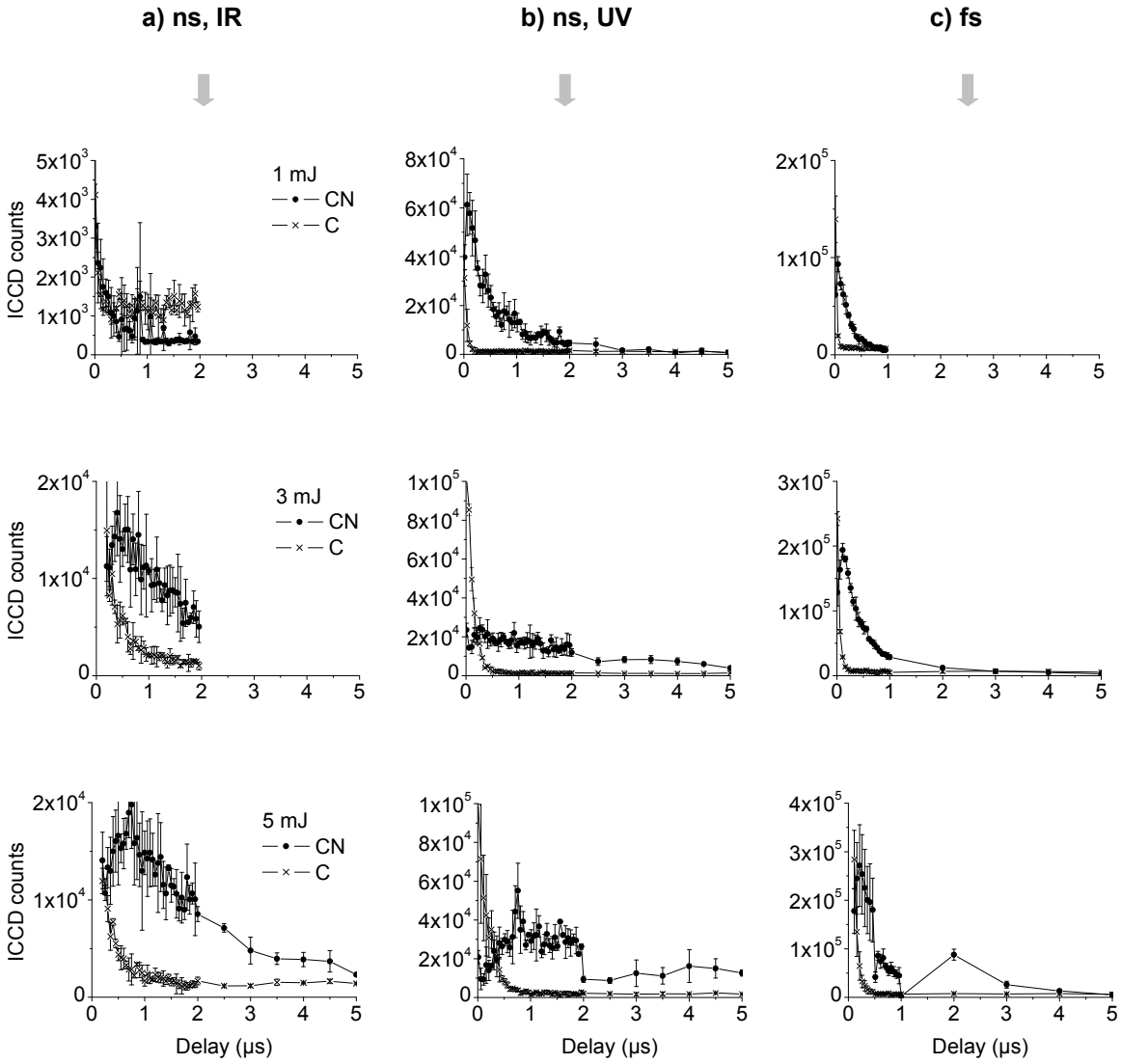

Fig. 4. Time evolutions of emissions of atomic carbon C and molecular radicals CN from plasmas induced by nanosecond IR (a), nanosecond UV (b), and femtosecond (c) laser pulses on the surface of a nylon sample with pulse energy of 1, 3 and 5 mJ.

In Fig. 4a we can see that for the nanosecond IR ablation, signal from CN molecules is rather weak for low laser energies. Efficient production of CN molecules is due to the recombination with ambient air. Such recombination becomes more important for high pulse energies. As we already see in the section 2.2 with shadowgraphs, for these energies, tailing part of laser pulse is strongly absorbed by the plasma. Absorption of laser energy by the plasma increases the temperature of the plasma, and in turn, its reaction rate with the ambient air due to an increased collision energy.[19] This observation leads to the conclusion that the nanosecond IR ablation regime is not suitable for analysis of organic materials using LIBS with molecular emission, because of its low efficiency to produce native molecular fragments and high rate of recombination with ambient air.

For the nanosecond UV ablation (Fig. 4b), we can see an efficient production of native CN molecules with weak laser energies. This production decreases when energy increases. The recombination with ambient air is observed for high laser energies. For low energy nanosecond UV ablations, the dominant process is photochemical ablation.[20] High energy of UV photon (4.66 eV) allows efficient photoionization of material and direct bond breaking leading to non thermal

ablation and efficient generation of molecular fragments.[21-23] When laser pulse energy is increased and as there is not shielding of laser pulse by plasma, energy coupled to the sample increases, leading to higher plasma temperature and higher atomization degree in the plasma due to photothermal process. Recombination with ambient air becomes important with respect to the production of native molecules. From these observations, we can conclude that low fluence nanosecond UV ablation is quite suitable for an efficient analysis of organic or biological materials with LIBS under atmospheric pressure by providing efficient molecular ablation and allowing low interference due to the recombination with ambient air.

For the femtosecond ablation, Fig. 4c shows efficient molecular ablation for all the three used energies with increasing initial molecular emission intensity for increasing pulse energy. For low pulse energies (1 and 3 mJ), the contribution from recombination is negligible. For 5 mJ, signal due to recombination can be observed for long delays. This is quite similar to the results obtained in the nanosecond UV ablation regime with however, a significantly higher production rate of native CN molecules. In fact, as already shown by the shadowgraphs, in femtosecond ablation, there is no post ablation interaction between plasma and laser pulse. And due to its high intensity, photochemical ablation is a dominant process through multiphoton ionization and direct bond breaking.[24] As for the nanosecond UV ablation, the femtosecond ablation also allows efficient LIBS analysis of organic and biological samples using molecular emission without interference due the recombination with atmospheric air.

3. DETECTION OF BACTERIA WITH MOLECULAR EMISSIONS OBSERVED IN ABLATION PLASMA

As an application of the optimized molecular fragment generation in the femtosecond ablation regime, in this section we show the discrimination of biological materials, bacteria for instance, using LIBS. Spectral signature of the emission from CN molecules will be used as a marker for biological materials.

3.1 Experimental setup

In our experiments, a CPA (Chirped Pulse Amplification) laser system provided 4.5 mJ, 120 fs and 810 nm pulses at a repetition rate of 20 Hz. Laser pulses were focused by a single lens of 30 mm focal length on the surface of the samples. The resulted beam waist was about 100 μm, resulting in a fluence of 14 J/cm^2. Samples were prepared according to the following process: growth of bacteria overnight in liquid Luria Broth at 37°C under aeration; impact by aspiration of 20 mℓ solution of bacteria on a filter; washing of the charged filter by 20 mℓ distilled water with the same aspiration process; indoor drying for about an hour. Nitrocellulose filters were finally used instead of silver filters, for two reasons, i) in the femtosecond regime, two photon-excited plasmon emission saturated the detector over the interested spectral range; ii) they are much cheaper and extensively used in biological and chemical analysis, and therefore closer to a realistic analytical environment for applications. However the use of an organic filter made differential measurements necessary. We observed in the same experimental conditions spectral signatures of a filter charged with bacteria, a filter charged with the nutrition medium (same preparation process as for bacteria-charged filter without bacteria growth), and an unexposed filter. The samples were fixed on a rotation stage. The speed of rotation was set to allow a fresh sample spot for each laser shot. Optical emission from laser-induced plasma was collected by a lens of 50 mm focal (f# = 2), and coupled, via an optical fibre, to an Echelle spectrometer equipped with an ICCD camera (Andor Technology, Mechelle and iStar).

3.2 Time-resolved LIBS for identification of native CN radicals form a biological sample

Three different types of samples have been used for this study: *Escherichia coli* bacteria (containing native CN bonds), a nitrocellulose filter (that contains nitrogen and carbon atoms as elementary constituents), and a pure graphite sample containing exclusively carbon rings. Time-integrated spectra of these samples showed similar spectra of the molecular bands of interest even if the intensity ratio of CN/C_2 varied from sample to sample. The results of time-resolved kinetic study on the intensity of CN (0-0) band head are presented in Fig. 5. The series of kinetic spectra have been recorded with an automatically shifted detection gate of 50 ns width. The step of the gate shift was 50 ns for a detection delay between 60 ns and 960 ns, and 500 ns for longer delays. For the graphite sample, CN bond formation due to recombination with ambient air is clearly observed. The band head intensity increases and reaches a maximum at a delay of 450 ns. This time constant is quite consistent with previously reported value for nanosecond ablation.[14] Dramatically different behaviour has been observed for either *Escherichia coli* or nitrocellulose filter. The band head intensity decays

rapidly for both of these two samples, with exponential decay time constant of (94 ± 20) ns for bacteria and (185 ± 35) ns for the filter. These results show that a carbon containing graphite sample can be distinguished unambiguously from an organic material containing simultaneously carbon and nitrogen or a biological sample which contains inevitably native CN bonds. The further distinction between the last two types of samples needs more precise quantitative comparison between decay time constants. Different samples ablated with different laser parameters could present different time constants. As shown by our result, we expect a shorter decay time constant for a biological sample than for an organic carbon and nitrogen containing sample since recombinations in the plasma between atomic carbon and nitrogen lead to a longer decay time constant. Precisely measured decay kinetics of the CN band provides thus a valuable molecular spectral signature of a biological medium.

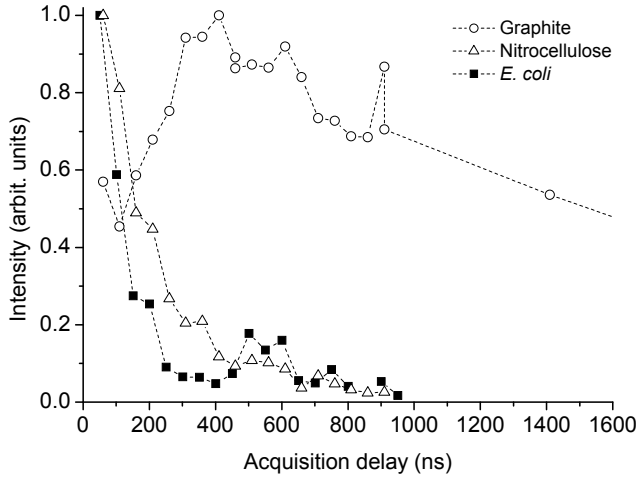

Fig. 5. Kinetics of the CN (0-0) band head intensity for graphite, nitrocellulose filter, and *Escherichia coli* bacteria. The signals are normalized for each sample (figure extracted from Ref. 9).

4. CONCLUSION

We have studied the early stage expansion and the subsequent molecular emission of the plasma induced on the surface of a nylon sample in different laser ablation regimes in terms of pulse duration, wavelength and fluence, in order to identify optimized ablation regimes for LIBS analysis of organic and biological materials under the atmospheric pressure. Our results demonstrate that an optimized ablation regime can be found with an efficient production of native molecular fragments and a minimized recombination with ambient air. This regime can be provided by either nanosecond UV pulses with low fluence or femtosecond pulses. Nanosecond IR laser is not suitable for organic material analysis using molecular emission, because there is a low molecule production rate at low fluence; and at high fluence the absorption of laser energy by the plasma lead to shielding of the pulse and heating of the plasma. We have observed the correlation between the LSD and the high rate of recombination with ambient air for this regime. For nanosecond UV laser pulses at high fluence, energy deposited on the sample increases because the absence of pulse shielding by the plasma. The important energy deposited on the sample increases the initial energy of the plasma which leads to a higher atomization degree and a reduced molecule production. The recombination rate with ambient air is also increased due to higher collision energies. For the femtosecond ablation, the recombination is observed at high laser energy, while the initial native molecular fragment production remains always high for increasing laser energy in this regime. Compared to the nanosecond ablations, the femtosecond regime offers the highest production rate of molecular fragments. However for application purposes, the use of a nanosecond UV laser with a much more compact and reliable system is obviously advantaged compared to a femtosecond laser who remains actually still more complicate to operate. The optimized femtosecond ablation regime has been applied to detection native CN radicals ablated from bacteria, which provides a signature of a biological material. Emission from CN radicals due to recombination with the atmospheric air can be distinguished with their specific time evolution behavior.

ACKNOWLEDGEMENTS

The authors thank the France Berkeley Funding for the supports.

REFERENCES

[1] Mizioley, A. W., Palleschi V., Schchter, I., [Laser-Induced Breakdown Spectroscopy (LIBS): Fundamentals and Applications], Cambridge (2006).
[2] Cremers, D. A., Radziemski, L. J., [Handbook of Laser-Induced Breakdown Spectroscopy], Wiley (2006).
[3] De Lucia, Jr., F. C., Harmon, R. S., McNesby, K. L., Wonkel, Jr., R. J. and Miziolek, A. W., "Laser-induced breakdown spectroscopy analysis of energetic materials" Appl. Opt. 42, 6148-6152 (2003).
[4] Lopez-Moreno, C., Palanco, S., Laserna, J. J., DeLucia Jr., F., Miziolek, A., Rose, J., Walter R. A. and Whitehouse, A. I., "Test of a stand-off laser-induced breakdown spectroscopy sensor for the detection of explosive residues on solid surfaces", J. Anal. At. Spectrom. 21, 55-60 (2006).
[5] Hybl, J. D., Lithgow, G. A. and Buckley, S.G., "Laser-Induced Breakdown Spectroscopy Detection and Classification of Biological Aerosols", Appl. Spectroscopy, 57, 1207-1215 (2003).
[6] Samuels, A. C., De Lucia, Jr., F.C., McNesby, K. L. and Miziolek, A. W., "Laser-induced breakdown spectroscopy of bacterial spores, molds, pollens, and protein: initial studies of discrimination potential", Appl. Opt. 42, 6205-6209 (2003).
[7] Morel, S., Leon, N., Adam, P. and Amouroux, "Detection of bacteria by time-resolved laser-induced breakdown spectroscopy", J., Appl. Opt. 42, 6184-6191 (2003).
[8] Baudelet, M., Yu, J., Bossu, M., Jovelet, J., Wolf, J.-P., Amodeo, T., Fréjafon, E., Laloi, P., "Discrimination of microbiological samples using femtosecond laser-induced breakdown spectroscopy", Appl. Phys. Lett. 89 163903 (2006).
[9] Baudelet, M., Guyon, L., Yu, J., Wolf, J. P., Amodeo, T., Fréjafon, E., Laloi, P., "Spectral signature of native CN bonds for bacterium detection and identification using femtosecond laser-induced breakdown spectroscopy", Appl. Phys. Lett. 88, 063901 (2006).
[10] Baudelet, M., Boueri, M., Yu, J., Mao, S. S., Piscitelli, V., Mao X. and Russo, R. E., "Time-resolved ultraviolet laser-induced breakdown spectroscopy for organic material analysis", Spectrochim. Acta B, 62 1329-1334 (2007).
[11] Baudelet, M., Guyon, L., Yu, J., Wolf, J. P., Amodeo, T., Fréjafon, E., Laloi, P., "Femtosecond time resolved laser-induced breakdown spectroscopy for detection and identification of bacteria : a comparison to the nanosecond regime", J. Appl. Phys. 99, 084701 (2006).
[12] Zel'dovich, Y.B. and Raizer, Y.P., [Physics of Shock Waves and High-Temperature Hydrodynamic Phenomena], Dover Publications (2002).
[13] Capitelli, M., Ferreira, C. M., Gordiets, B. F. and Osipov, A. I., [Plasma Kinetics in Atmospheric Gases], Springer (2000).
[14] Vivien, C., Hermann, J., Perrone, A., Boulmer-Leborgne, C. and Luches, A., "A study of molecule formation during laser ablation of graphite in low-pressure nitrogen", J. Phys. D 31, 1263-1272 (1998).
[15] St-Onge, L., Sing, R., Béchard, S. and Sabsabi, M., "Carbon emissions following 1.064 μm laser ablation of graphite and organic samples in ambient air", Appl. Phys. A: Mater. Sci. Process. 69, S913-S916 (1999).
[16] Abdelli-Messaci, S., Kerdja, T., Bendib, A. and Malek, "Emission study of C_2 and CN in laser-created carbon plasma under nitrogen environment", S., J. Phys. D 35, 2772-2778 (2002).
[17] Thareja, R. K., Dwivedi, R. K. and Ebihara, K., "Interaction of ambient nitrogen gas and laser ablated carbon plume: Formation of CN", Nucl. Instr. and Meth. in Phys. Res. B, 192, 301 (2002).
[18] Trusso, S., Barletta, E., Barreca, F. and Neri, F., "Pulsed laser ablation of SiC in a nitrogen atmosphere: formation of CN", Appl. Phys. A 79, 1997-2005 (2004).
[19] Hochstim, A.R., [Kinetic processes in gases and plasmas], Academic Press (1969).
[20] Bäuerle, D., [Laser Processing and Chemistry], 3th edition, Springer (2000).
[21] Bityurin, N., Luk'yanchuk, B. S., Hong, M. H. and Chong, T. C., "Models for laser ablation of polymers", Chem. Rev. 103, 519-552 (2003).
[22] Lippert, T. and Dickinson, J. T., "Chemical and Spectroscopic Aspects of Polymer Ablation: Special Features and Novel Directions", Chem. Rev., 103, 453-485 (2003).

[23] Kuhnke, M., Cramer, L., Dyer, P. E., Dickinson, J. T., Lippert, T., Niino, H., Pervolaraki, M., Walton, C. D., Wokaun, A., "F2 excimer laser (157 nm) ablation of polymers: relation of neutral and ionic fragment detection and absorption", Journal of Physics: Conference series 59, 625-631 (2007).
[24] Bonse, J., Baudach, S., Krüger, J., Kautek, W., Lenzner, M., "Femtosecond laser ablation of silicon–modification thresholds and morphology", Appl. Phys. A 74, 19-25 (2002).